2018 Annual American Control Conference (ACC)
June 27–29, 2018. Wisconsin Center, Milwaukee, USA

A Time-Warping Transformation for Time-Optimal Movement in Differentially Flat Systems*

Marcus Greiff[1]

***Abstract*— The notion of warping the rate of time is explored in the context of differentially flat systems to enable time-optimal motion by convex optimisation. Examples are given with systems configured on the special Euclidean groups $SE(2)$ and $SE(3)$, with and without differential constraints. The proposed method complements classical methods of motion planning, may be used in a real-time context with guarantees on time-optimality subject to constraints on the first two derivatives on the flat output trajectory and all time-warping derivatives. In addition, an iterative method is presented to find close-to-optimal solutions in the event of non-convex constraints.**

I. Introduction

Optimal motion planning of nonlinear rigid body dynamics, such as the unmanned aerial vehicle (UAV) or the unmanned ground vehicles (UGV), is a well studied field due to its difficulties and utilities. The scientific literature is rich with ideas, often involving graph search methods [1], combinatorial methods [2], or recent advances in convex optimisation to drive the systems to some terminal state while minimising an objective function $J(\mathbf{x}(t), \mathbf{u}(t), t_f)$ for some terminal time t_f. Many state-of-the-art algorithms are based on the receding horizon principle, using linear quadratic theory (LQ) or model predictive control approaches (MPC) to find optimal state trajectories, see e.g. [3]–[5]. Interesting approaches include extensions of the RRT algorithms [6], such as the promising CL-RRT [7], [8]. Similar methods are employed in the growing of graphs in the LQR-tree algorithms [9], using the with LQ-theory to find a piecewise linear feedback law which minimises $J(\mathbf{x}(t), \mathbf{u}(t), t_f)$.

Regardless of the approach taken, it is often necessary to make a set of simplifying assumptions to retain computational feasibility and make statements of optimality. In the mentioned methods, this motivates approximations of the nonlinear dynamics by linear time-invariant (LTI) systems

$$\dot{\mathbf{x}}(t) = \mathbf{A}\mathbf{x}(t) + \mathbf{B}\mathbf{u}(t), \tag{1}$$

through linearization at a single point in the state-space, along a state trajectory in the LQR-tree case [9], or as piecewise linear systems in partitions of the state-space, commonly referred to as explicit MPC methods, see e.g. [10]. However, if only considering differentially flat systems no such approximations are needed. There exist radically different approaches, such as the convex polynomial optimisation (CPO) [11], which finds a set of polynomial splines subject to end-point conditions. The method has been shown to outperform the RRT*-approach for UAV planning [12], only incorporating constraints on the spline derivatives and ascribing each spline with a fixed time to retain convexity. As such, it is very difficult to make statements about time-optimality in any CPO method.

In this paper, we present a receding horizon approach to time-optimal motion planning of differentially flat systems, compatible with prior mentioned CPO- and MPC-methods. The paper first recapitulates the concept of differential flatness and defines the considered systems in Section III, before introducing the concept of time-warping in Section IV. To show the generality of the approach, we give two numerical examples in Section VII pertaining to different UGV and UAV systems configured on the matrix Lie groups $SE(2)$ and $SE(3)$, respectively. The presented methods avoid the pre-mentioned LTI-simplification of the nonlinear system by invoking the property of differential flatness, forming a complementary quadratic program based on the time-warping of the reference trajectory on a parallel time-line.

II. Problem formulation

Given a feasible flat-output trajectory $\boldsymbol{\gamma}(t)$, which drives the system from an initial state $\mathbf{x}(t_0)$ to a terminal state $\mathbf{x}(t_f)$, find a time optimal trajectory, $\boldsymbol{\gamma}^*(t)$, which minimises t_f by altering the derivatives of $\boldsymbol{\gamma}(t)$ such that a set of constraints are met at all times on which $\boldsymbol{\gamma}^*(t)$ is defined. The method should (1) not implement any LTI approximations of the nonlinear system as is required in standard MPC-methods and (2) make guarantees at all times, not just at the end-points as with the CPO or other spline-based methods.

III. Preliminaries

For future reference, any rigid-body is defined in a Cartesian body frame $\{\mathcal{B}\}$ relating to a global coordinate frame $\{\mathcal{G}\}$ by a rotation and translation. Vectors defined in each frame are sub-indexed $(\cdot)_\mathcal{B}$ and $(\cdot)_\mathcal{G}$, and the orthonormal basis vectors spanning $\mathbb{R}^3$ in the body and global coordinate systems by $\{\mathbf{x}_\mathcal{B}, \mathbf{y}_\mathcal{B}, \mathbf{z}_\mathcal{B}\}$ and $\{\mathbf{x}_\mathcal{G}, \mathbf{y}_\mathcal{G}, \mathbf{z}_\mathcal{G}\}$ respectively.

A. Differential Flatness

The property of differential flatness was first introduced in a differential algebraic setting [13], and has more recently been explored using in Lie-Bäckman transformation theory [14]. Prior results on the mechanical rigid-body control systems considered in this paper are found in [15]–[17].

*The research leading to these results has received funding from the Swedish Science Foundation (SSF) project "Semantic mapping and visual navigation for smart robots" (RIT15-0038). Dept. of Automatic Control, LTH, Lund University, SE-221 00 Lund, Sweden. The author is a member of the Lund Center for Control of Complex Engineering Systems (LCCC) funded by the Swedish Research Council (VR) and the Excellence Center Linköping - Lund in Information Technology (ELLIIT).

[1]Marcus Greiff is with the Department of Automatic Control, Lund University, Lund, Sweden marcus.greiff@control.lth.se

Definition 1 ([13]): A nonlinear system, $\dot{\mathbf{x}} = \mathbf{f}(\mathbf{x}, \mathbf{u})$, with a state vector $\mathbf{x} \in \mathbb{R}^n$, $\mathbf{u} \in \mathbb{R}^m$, where $\mathbf{f}$ a smooth vector field is called differentially flat if there exists a set of flat outputs $\boldsymbol{\gamma} \in \mathbb{R}^m$,

$$\boldsymbol{\gamma} = \mathbf{h}(\mathbf{x}, \mathbf{u}, \dot{\mathbf{u}}, \cdots, \mathbf{u}^{(r)}), \tag{2}$$

such that

$$\mathbf{x} = \boldsymbol{\phi}(\boldsymbol{\gamma}, \dot{\boldsymbol{\gamma}}, \cdots, \boldsymbol{\gamma}^{(q)}), \tag{3}$$

$$\mathbf{u} = \boldsymbol{\beta}(\boldsymbol{\gamma}, \dot{\boldsymbol{\gamma}}, \cdots, \boldsymbol{\gamma}^{(q)}), \tag{4}$$

where $\{\mathbf{h}, \boldsymbol{\phi}, \boldsymbol{\beta}\}$ are smooth functions.

Remark 1: By Definition 1, the computation of all system states and control signals from the flat outputs $\boldsymbol{\gamma}$ may be done at any point in time without integration. In addition, the behaviour of the nonlinear system in this flat output space is that of a multidimensional multiple-order integrator.

B. Torque-controlled SE(2) configured UGV

Consider first the differentially torque-driven UGV, defined by the scalar parameters $h, r, J, m \in \mathbb{R}^+$ and controlled by two time-varying torques $\tau_1(t), \tau_2(t) \in \mathbb{R}$ generated by the wheels as illustrated in Figure 1.

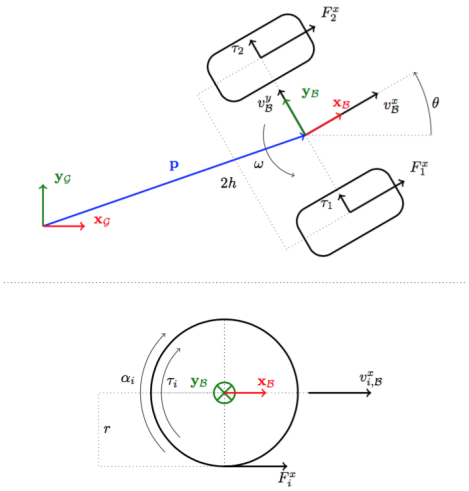

Fig. 1. *Top:* An $SE(2)$ rigid-body. *Bottom:* Wheel forces.

The rigid-body is configured on $\mathbf{g}(\mathbf{p}, \theta) \in SE(2)$, where $\mathbf{p} = [p_{\mathcal{G}}^x, p_{\mathcal{G}}^y]$ defines the position of the body frame origin in the global frame. For this $SE(2)$ body, the one-parametric group $\boldsymbol{\xi} = \begin{bmatrix} \omega & v_{\mathcal{B}}^x & v_{\mathcal{B}}^y \end{bmatrix}$ defines an element of the Lie algebra $[\boldsymbol{\xi}]^\wedge \in \mathfrak{se}(2)$. Letting,

$$\mathbf{x} = \begin{bmatrix} \theta & p_{\mathcal{G}}^x & p_{\mathcal{G}}^y & \omega & v_{\mathcal{B}}^x & v_{\mathcal{B}}^y \end{bmatrix}^T, \quad \mathbf{u} = \begin{bmatrix} \tau_1 & \tau_2 \end{bmatrix}^T, \tag{5}$$

the Newton-Euler equations yield the dynamical system

$$\dot{\theta}(t) = \omega_{\mathcal{B}}(t) \tag{6a}$$

$$\dot{p}_{\mathcal{G}}^x(t) = v_{\mathcal{B}}^x(t)\cos(\theta(t)) - v_{\mathcal{B}}^y(t)\sin(\theta(t)) \tag{6b}$$

$$\dot{p}_{\mathcal{G}}^y(t) = v_{\mathcal{B}}^x(t)\sin(\theta(t)) + v_{\mathcal{B}}^y(t)\cos(\theta(t)) \tag{6c}$$

$$\dot{\omega}(t) = (h/(Jr))(\tau_1(t) - \tau_2(t)) \tag{6d}$$

$$\dot{v}_{\mathcal{B}}^x(t) = \omega(t)v_{\mathcal{B}}^y(t) + (r/m)(\tau_1(t) + \tau_2(t)) \tag{6e}$$

$$\dot{v}_{\mathcal{B}}^y(t) = -\omega(t)v_{\mathcal{B}}^x(t) \tag{6f}$$

Notably, (6) can be written in a controlled Euler-Poincaré form with an associated tensor $\mathbb{I} = \text{diag}\{J, m, m\}$, whereby the controllability in an STLCC sense can be proven when $\tau_1 \neq \pm\tau_2$ [16]. In addition, differential flatness can be shown with the position of the centre of mass, defining

$$\boldsymbol{\gamma}(t) = \mathbf{h}(\mathbf{x}(t)) = \begin{bmatrix} p_{\mathcal{G}}^x(t) & p_{\mathcal{G}}^y(t) \end{bmatrix}^T \in C^3(\mathbb{R}^2), \tag{7}$$

with the functions $\mathbf{x}(t) = \boldsymbol{\phi}(\cdot)$ and $\mathbf{u}(t) = \boldsymbol{\beta}(\cdot)$ given in a complementary technical report [18]. Notably, the maps defining the flatness equations are smooth if and only if $\tau_1 \neq \pm\tau_2$, with the equations becoming extremely poorly conditioned close to the singularity. Such singularities are common in mechanical control systems and relate to the prior results of controllability, as an uncontrollable system cannot be differentially flat by definition.

C. Torque-Controlled UGV with Differential Constraints

If subjecting the $SE(2)$ configured UGV to non-holonomic constraints, prohibiting any movement in the $\mathbf{y}_{\mathcal{B}}$-direction we need to reformulate the dynamics slightly to incorporate the wheel speeds $\alpha_1(t), \alpha_2(t) \in \mathbb{R}$ in the model. Writing the state- and control signal vectors

$$\mathbf{x} = [x_i] = [p_{\mathcal{G}}^x, p_{\mathcal{G}}^y, \theta, \dot{\alpha}_1, \dot{\alpha}_2]^T, \quad \mathbf{u} = [u_i] = [\tau_1, \tau_2]^T, \tag{8}$$

and subjecting the system to condition of no lateral slip, the body adheres to the non-holonomic constraints

$$A(\mathbf{x})\dot{\mathbf{x}} = \begin{bmatrix} \sin(x_3) & -\cos(x_3) & 0 & 0 & 0 \\ \cos(x_3) & \sin(x_3) & 0 & -r/2 & -r/2 \\ 0 & 0 & 1 & -1/(2h) & 1/(2h) \end{bmatrix} \dot{\mathbf{x}}, \tag{9}$$

whereby Newton's second law results in

$$\dot{p}_{\mathcal{G}}^x(t) = (\dot{\alpha}_1(t) + \dot{\alpha}_2(t))(r/2)\cos(\theta) \tag{10a}$$

$$\dot{p}_{\mathcal{G}}^y(t) = (\dot{\alpha}_1(t) + \dot{\alpha}_2(t))(r/2)\sin(\theta) \tag{10b}$$

$$\dot{\theta}(t) = (\dot{\alpha}_2 - \dot{\alpha}_1(t))/(2h) \tag{10c}$$

$$\ddot{\alpha}_1(t) = J_1^{-1}\tau_1(t) \tag{10d}$$

$$\ddot{\alpha}_2(t) = J_2^{-1}\tau_2(t) \tag{10e}$$

This system does not admit an Euler-Poincaré form, and must instead be analysed using the Lie algebra rank condition (LARC) presented in [19]. A closed strong accessibility algebra may be found and small time controllability proven for $\mathbf{x}(t) \in \mathbb{R}^5 \backslash \{\alpha_1 = 0 \wedge \alpha_2 = 0\}$ [18]. Writing (10) in terms of Pfaffian constraints by the methodology outlined in [15], the system is found to be differentially flat on

$$\boldsymbol{\gamma}(t) = \mathbf{h}(\mathbf{x}(t)) = \begin{bmatrix} p_{\mathcal{G}}^x(t) & p_{\mathcal{G}}^y(t) \end{bmatrix}^T \in C^2(\mathbb{R}^2), \tag{11}$$

requiring less smooth curves in the flat output space than the unconstrained model, with the maps $\mathbf{x}(t) = \boldsymbol{\phi}(\cdot)$ and $\mathbf{u}(t) = \boldsymbol{\beta}(\cdot)$ derived and presented in detail in [18]. Just as in the unconstrained case, the maps admit singularities, being smooth if and only if $||\dot{\boldsymbol{\gamma}}|| \neq 0$, again relating the flatness equations to results on controllability.

D. Rotor-Speed Controlled SE(3)-Configured UAV

The quadcopter UAV has been the subject of much study, and the reader is referred to [20] for a formal derivation of the $SE(3)$-configured rigid-body dynamics. The body is moved by applying a set of forces $\mathbf{f}(t) = [f_x(t), f_y(t), f_z(t)]$ and torques $\boldsymbol{\tau}(t) = [\tau_x(t), \tau_y(t), \tau_z(t)]$ in the body frame, with $f_x = f_y = 0\ \forall t$ due to the rotor configuration (see Figure 2).

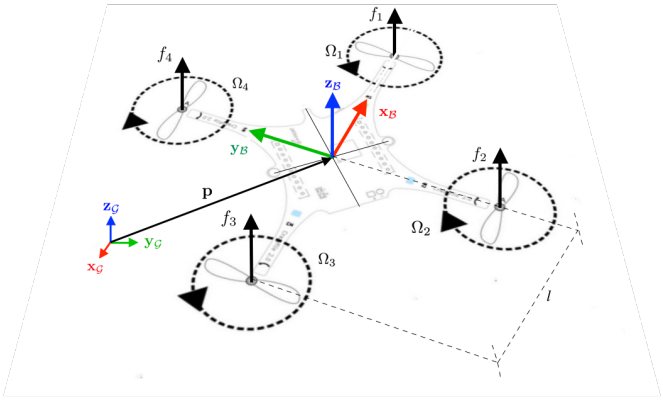

Fig. 2. The $SE(3)$ configured UAV system.

In this rotor-speed controlled UAV, forces and torques f_i, τ_i generated by a rotor i at a rotor speed Ω_i are given by

$$f_i(t) \approx k\Omega_i^2(t), \qquad \tau_i(t) \approx b_i\Omega_i^2(t) + I_M\dot{\Omega}_i(t). \tag{12}$$

The approximations, which are motivated by blade element theory in [21] and experimentally verified in [22], give rise to a map from rotor speeds to thrust by

$$\begin{bmatrix} f_z(t) \\ \tau_x(t) \\ \tau_y(t) \\ \tau_z(t) \end{bmatrix} = \begin{bmatrix} k\sum_{i=1}^4 \Omega_i^2(t) \\ kl(-\Omega_2^2(t) + \Omega_4^2(t)) \\ kl(-\Omega_1^2(t) + \Omega_3^2(t)) \\ \sum_{i=1}^4 b\Omega_i^2(t) + I_M\dot{\Omega}_i(t) \end{bmatrix}. \tag{13}$$

If making the additional assumption $I_M \approx 0$ and $\Omega_i(t) > 0$, the map from rotor speeds to rigid-body forces (13) is both smooth and surjective. Consequently, controllability may be shown using Theorem 2.1 in [16] and differential flatness may be proven, with the flat output space constituted by the global position, $\mathbf{p} = \begin{bmatrix} p_G^x(t) & p_G^y(t) & p_G^z(t) \end{bmatrix}$, and a parametrisation of the rotation about the body z-axis, $\psi(t)$. Similar to the previous two systems, the flat outputs

$$\boldsymbol{\gamma}(t) = \mathbf{h}(\mathbf{x}(t)) = \begin{bmatrix} x_G(t) & y_G(t) & z_G(t) & \psi(t) \end{bmatrix}^T \in C^3(\mathbb{R}^4). \tag{14}$$

and the corresponding maps $\boldsymbol{\phi}(\cdot)$ and $\boldsymbol{\beta}(\cdot)$ remain smooth if $\ddot{\gamma}_1^2 + \ddot{\gamma}_2^2 + (\ddot{\gamma}_3 - g)^2 \neq 0$, with g being the gravitational constant. The maps are omitted for brevity but presented in [23] using a Tait-Bryan parametrisation of the rotation, and explicitly stated in [22] using the quaternion formalism.

E. Dynamical Constraints

It should be noted that the systems in Sections III-B-III-D reside on an unconstrained state-space. In a real-time context, the states and control signal vectors will be defined on subsets of $\mathbb{R}^n$ and $\mathbb{R}^m$ respectively. To analyse how the saturations affect the flat output space, we consider two forms of saturation functions with time-varying vector input $[v_i(t)] = \mathbf{v}(t)$ and output $[w_i(t)] = \mathbf{w}(t)$. The first is a rectangular saturation with time-varying upper and lower bounds $[w_{+,i}(t)] = \mathbf{w}_+(t), [w_{-,i}(t)] = \mathbf{w}_-(t)$ on the form

$$\mathbf{w}(t) = \text{sat}_{l_1}(\mathbf{v}(t)) = \begin{cases} w_{+,i}(t) & \text{if } v_i(t) > w_{+,i}(t) \\ w_{-,i}(t) & \text{if } v_i(t) < w_{-,i}(t) \\ v_i(t) & \text{otherwise} \end{cases} \tag{15}$$

And the second is an spherical saturation defined by a scalar bound $v^r(t) > 0$

$$\mathbf{w}(t) = \text{sat}_{l_2}(\mathbf{v}(t)) = \begin{cases} \mathbf{v}(t) & \text{if } ||\mathbf{v}(t)||_2 \leq w_r(t) \\ w_r(t)\frac{\mathbf{v}(t)}{||\mathbf{v}(t)||_2} & \text{if } ||\mathbf{v}(t)||_2 > w_r(t) \end{cases} \tag{16}$$

When considering these functions in an optimisation context, we note that the output $\mathbf{w}(t)$, subject to the saturations (15) (16), at all times satisfies constraints on the form

$$\boldsymbol{\sigma}(\mathbf{w}(t)) = \begin{cases} w_i(t) - w_{+,i}(t) & \leq 0 \\ -w_i(t) + w_{-,i}(t) & \leq 0 \\ ||\mathbf{w}(t)||_2 - w_r(t) & \leq 0 \end{cases}. \tag{17}$$

.

IV. A Warping Transformation of Time

In this section we assume knowledge of a trajectory in flat output space $\boldsymbol{\gamma}(\tau)$. From the controllability analysis, the considered systems are flat on $\mathbf{x}(t) \in \mathbb{R}^n$ and may follow any $\boldsymbol{\gamma}(\tau) \in C^M(\mathbb{R}^m)$ of sufficient smoothness. Efficient ways of generating such trajectories have been presented in the MPC- and CPO-methods referenced in the introduction [3]–[5], [11]. We consider these flat output trajectories as a shape functions and introduce the notion of time-warping, inspired in part by the path variable and approaches in [24]–[26]. For future reference, we denote derivatives of a time-varying function $\mathbf{w}(t, \tau)$ with respect to τ by

$$\frac{d^i\mathbf{w}(t,\tau)}{d\tau^i} = D_\tau^i\mathbf{w}(t,\tau) = \mathbf{w}_\tau^{(i)}(t,\tau). \tag{18}$$

Definition 2: Let a trajectory $\boldsymbol{\gamma}(\tau)$ be generated in terms of the time unit τ, relating to a second time unit t on which the system evolves, such that $\alpha(\tau)d\tau = dt$ for some integrable $\alpha(\tau) > 0$, with

$$t_1 = \int_0^{t_1} 1dt = \int_0^{t_1} \alpha(\tau)d\tau. \tag{19}$$

by the integrability of $\alpha(\tau)$.

The definition, illustrated in Figure 3, is useful in the sense that it allows for slowing and fastening of movement along $\boldsymbol{\gamma}(\tau)$ by the variation of $\alpha(\tau)$, effectively allowing higher order derivatives of the trajectory $\boldsymbol{\gamma}(\tau)$ to be confined within certain set bounds, corresponding to physical saturations of the differentially flat system (17).

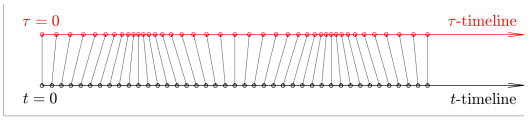

Fig. 3. Relation between τ and t with a sinusoidal $\alpha(\tau)$.

To demonstrate the idea, consider a generalisation of the chain rule known as Faá di Bruno's formula,

$$D_t^n f(g(t)) = \sum \frac{n!}{k_1! \cdots k_n!} (D_t^k f)(g(t)) \Big(\frac{D_t^1 g(t)}{1!}\Big)^{k_1} \cdots \Big(\frac{D_t^n g(t)}{n!}\Big)^{k_n} \tag{20}$$

where $k = k_1 + \cdots + k_n$, and the sum is over all partitions of n, as derived by [27]. This result shows exactly how $\alpha(\tau)$ and its derivatives affect the trajectory as seen on the t-timeline. It should be noted that the condition of simple integrability of $\alpha(\tau)$ does not generate sufficiently smooth, hence followable trajectories $\boldsymbol{\gamma}(t)$ on the t-timeline. Instead, we require a stronger condition of smoothness, visible from (20) as $\alpha(\tau) \in C^{M-1}(\mathbb{R}^m)$ and summarised in the following theorem.

Theorem 1: Any flat output trajectory $\gamma(\tau) \in C^M$ defined on the τ-timeline by Definition 2, such that $\alpha(\tau)d\tau = dt$, may be followed on the t-timeline with $\gamma(t) \in C^M$ if $\alpha(\tau) \in C^{M-1}$.

Proof: Let $A(\tau)$ denote the primitive function of $\alpha(\tau)$ with $A(0) = 0$ by consequence of (19). From the fundamental theorem of calculus and Definition 2, we find

$$t = \int_0^t \alpha(\tau)d\tau = A(\tau) - A(0) = A(\tau). \tag{21}$$

Consequently, any trajectory on the t-timeline may be written $\boldsymbol{\gamma}(t) = \boldsymbol{\gamma}(A(\tau))$. As $\boldsymbol{\gamma}(\tau) \in C^M \Leftrightarrow d^M\boldsymbol{\gamma}(\tau)/d\tau^M \in C^0$, we note that $d^M\boldsymbol{\gamma}(A(\tau))/dt^M \in C^0$, making the trajectory feasible on the t-timeline, if $A(\tau) \in C^M \Rightarrow \alpha(\tau) \in C^{M-1}$ by Faá di Bruno's formula (20). ∎

V. Problem Formulation Revisited

With prior definitions, consider a differentially flat system with corresponding state- and control signal vector $\{\mathbf{x}(\tau), \mathbf{u}(\tau)\}$ with surjective, smooth maps $\{\mathbf{h}(\cdot), \boldsymbol{\phi}(\cdot), \boldsymbol{\beta}(\cdot)\}$, for which there exists a known followable trajectory $\boldsymbol{\gamma}(\tau) \in C^M$ defined on $\tau \in [0, \tau_f]$, $\tau_f > 0$. The problem of finding a time-optimal trajectory of a system evolving on the t-timeline is then equivalent to maximising $\alpha(\tau) \in C^{M-1}, \tau \in [0, \tau_f]$, subject to constraints on $\alpha(\tau)$.

VI. A MPC Approach to Time-Optimality

In devising an efficient optimisation program to find $\alpha(\tau)$ and solve the problem, the formulation must include

(i) Conditions for smoothness by Theorem 1,
(ii) An objective function maximising $\alpha(\tau)$ $\forall \tau \in [0, \tau_f]$,
(iii) Constraints on $\boldsymbol{\sigma}(\alpha_\tau^{(i)}(\tau)) \leq 0 \quad i \in \{0, \cdots, M-1\}$,
(iv) Constraints on $\boldsymbol{\sigma}(\boldsymbol{\gamma}_t^{(i)}(\tau)) \leq 0 \quad i \in \{1, \cdots, M\}$,
(v) Constraints on $\boldsymbol{\sigma}(\mathbf{x}(\tau)) \leq 0$,
(vi) Constraints on $\boldsymbol{\sigma}(\mathbf{u}(\tau)) \leq 0$.

We will next go through the points (i)-(vi), detailing how they may be incorporated in an optimisation framework.

(i) Smoothness

To comply with the smoothness condition, it is clear that for a bounded input $u(\tau) \in C^0$,

$$D_\tau^{M-1}\alpha(\tau) = u(\tau) \in C^0 \Rightarrow \alpha(\tau) \in C^{M-1}. \tag{22}$$

Such a chain of integrators may be expressed as an LTI system with a state vector

$$\mathbf{x}_\alpha(t) = \begin{bmatrix} \alpha(\tau) & \alpha_\tau^{(1)}(\tau) & \cdots & \alpha_\tau^{(M-2)}(\tau) \end{bmatrix}^T \in \mathbb{R}^{M-1}, \tag{23}$$

and then discretised for some time step $\Delta\tau \ll \tau_f$ as

$$\mathbf{x}_\alpha(\Delta\tau(k+1)) = \mathbf{A}\mathbf{x}_\alpha(\Delta\tau k) + \mathbf{B}u(\Delta\tau k). \tag{24}$$

Forming a lifted system with a coarseness $N = \lceil \tau_f/\Delta\tau \rceil$,

$$\mathcal{X} = \begin{bmatrix} \mathbf{x}_\alpha(0\Delta\tau) \\ u(0\Delta\tau) \\ \vdots \\ \mathbf{x}_\alpha(N\Delta\tau) \\ u(N\Delta\tau) \end{bmatrix}, \; \mathcal{A} = \begin{bmatrix} -\mathbf{I} & \mathbf{0} & \mathbf{0} & \cdots & \mathbf{0} & \mathbf{0} \\ \mathbf{A} & \mathbf{B} & -\mathbf{I} & \cdots & \mathbf{0} & \mathbf{0} \\ \vdots & \vdots & \ddots & \ddots & \vdots & \vdots \\ \mathbf{0} & \mathbf{0} & \cdots & \mathbf{0} & \mathbf{A} & \mathbf{B} \end{bmatrix}, \tag{25}$$

the condition of smoothness may be written $\mathcal{A}\mathcal{X} = \mathbf{0}$.

(ii) The objective function: The convex objective function should keep $\alpha(\tau)$ as close as possible to a time-varying upper bound, while simultaneously minimising any higher derivatives of $\alpha(\tau)$. Defining a positive definite weight matrix $0 \prec \mathbf{Q} \in \mathbb{R}^{M\times M}$, this may be accomplished on each discrete time step $\Delta\tau k$ by minimising the quadratic form

$$\begin{bmatrix} \alpha_\tau^{(0)}(\Delta\tau k) - \alpha_+^{(0)}(\Delta\tau k) \\ \alpha_\tau^{(1)}(\Delta\tau k) \\ \vdots \\ \alpha_\tau^{(M-2)}(\Delta\tau k) \\ u(\Delta\tau k) \end{bmatrix}^T \mathbf{Q} \begin{bmatrix} \alpha_\tau^{(0)}(\Delta\tau k) - \alpha_+^{(0)}(\Delta\tau k) \\ \alpha_\tau^{(1)}(\Delta\tau k) \\ \vdots \\ \alpha_\tau^{(M-2)}(\Delta\tau k) \\ u(\Delta\tau k) \end{bmatrix}. \tag{26}$$

Similar to standard LQ-theory, the matrix $\mathbf{Q} = [q_{ij}]$, defines characteristics of the found solutions in terms of punishing deviations in the states $\mathbf{x}_\alpha$. Often, it is desirable to keep the system derivatives small to make movement less volatile, but letting $q_{11} = 1$, $q_{ij} = 0 \forall (i,j) \backslash \{i = 1 \wedge j = 1\}$ results in the most aggressive changes possible in $\alpha(\tau)$ while still conforming to the smoothness condition.

To write (26) in terms of the lifted system vector, $\mathcal{X}$, define a unit row-vector with the $(i+1)^{th}$ element set to 1,

$$\mathbf{p}^{(i)} = \begin{bmatrix} \underbrace{0}_{1} & \cdots & \underbrace{0}_{i} & \underbrace{1}_{i+1} & \underbrace{0}_{i+2} & \cdots & \underbrace{0}_{M} \end{bmatrix} \in \mathbb{R}^{1\times M} \tag{27}$$

allowing the formation of a matrix $\mathcal{P}^{(i)} = \mathbf{I}_N \otimes \mathbf{p}^{(i)}$ using the Kronecker product. Applying this operator to the lifted

state vector $\mathcal{X}$ effectively extracts certain derivatives of the discretised $\alpha(\tau)$, as by this definition

$$\mathcal{P}^{(i)}\mathcal{X} = \begin{bmatrix} \alpha_\tau^{(i)}(0\cdot\Delta\tau) & \alpha_\tau^{(i)}(1\cdot\Delta\tau) & \cdots & \alpha_\tau^{(i)}(N\cdot\Delta\tau) \end{bmatrix}^T. \tag{28}$$

Knowing the upper bound on $\alpha(\tau)$, previously defined as $\alpha_+^{(0)}(\tau)$, we write this constraint evaluated in discrete time

$$\bar{\boldsymbol{\alpha}}_+^{(0)} \triangleq \begin{bmatrix} \alpha_+^{(0)}(0\cdot\Delta\tau) & \alpha_+^{(0)}(1\cdot\Delta\tau) & \cdots & \alpha_+^{(0)}(N\cdot\Delta\tau) \end{bmatrix}^T, \tag{29}$$

and form a lifted positive definite weight matrix $0 \prec \mathcal{Q} = \mathbf{I}_N \otimes \mathbf{Q}$. The complete convex objective function is then

$$J(\mathcal{X}) = [\mathcal{X} - (\mathcal{P}^{(0)})^T\bar{\boldsymbol{\alpha}}_+^{(0)}]^T\mathcal{Q}[\mathcal{X} - (\mathcal{P}^{(0)})^T\bar{\boldsymbol{\alpha}}_+^{(0)}] \tag{30}$$

$$\triangleq \mathcal{X}^T\mathcal{Q}\mathcal{X} - 2(\bar{\boldsymbol{\alpha}}_+^{(0)})^T\mathcal{P}^{(0)}\mathcal{Q}\mathcal{X} \tag{31}$$

where the constant term may be dropped, as it only affects the value of $J(\mathcal{X})$ and not the found time-warping $\alpha(\tau)$.

(iii) Convex constraints in $\alpha(\tau)$: The constraints in $\alpha(\tau)$ are convex in $\mathcal{X}$ and may be included in the QP-formulation as defined in (17), such that

$$\min_{\mathcal{X}} \left(\mathcal{X}^T\mathcal{Q}\mathcal{X} - 2(\bar{\boldsymbol{\alpha}}_+^{(0)})^T\mathcal{P}(0)\mathcal{Q}\mathcal{X}\right) \tag{32a}$$

$$\text{subject to} \tag{32b}$$

$$\mathcal{A}\mathcal{X} = \mathbf{0} \tag{32c}$$

$$\boldsymbol{\sigma}(\alpha_\tau^{(0)}(\tau)) \leq \mathbf{0} \tag{32d}$$

$$\vdots$$

$$\boldsymbol{\sigma}(\alpha_\tau^{(M-1)}(\tau)) \leq \mathbf{0} \tag{32e}$$

To show the validity of the formulation (32) and hint where the reasoning is going, consider finding an $\alpha(\tau) \in C^5$ with a set of bounds

$$\alpha_+^{(0)}(\tau) = \cos(\tau)\sin(0.4\tau) + 10 + 2\sin(0.8\tau)\text{sign}(\cos(0.6\tau))$$
$$\alpha_-^{(0)}(\tau) = 0$$
$$\alpha_+^{(1)}(\tau) = 4 + \sin(\tau)$$
$$\alpha_-^{(1)}(\tau) = -\alpha_+^{(1)}(\tau)$$
$$\alpha_+^{(2)}(\tau) = 10 + 6\cos(\tau)\sin(3\tau) + 4\text{sign}(\sin(\tau))$$
$$\alpha_-^{(2)}(\tau) = -\alpha_+^{(2)}(\tau)$$

As shown in Figure 4, the computed time-warping $\alpha(\tau)$ is smooth and maximised within the defined feasible region

The significance of this result is that if there exists a followable trajectory $\boldsymbol{\gamma}(\tau) \in C^6$ to some hypothetical differentially flat system, such as the constrained UGV system (6), then the found $\alpha(\tau) \in C^5$ defines a modified trajectory $\boldsymbol{\gamma}^*(t)$ which is also followable on the t-timeline by Theorem 1 and optimal with respect to the constraints on $\alpha(\tau)$. The traversal of this modified trajectory takes $t_f = 4.6390$ $[s]$, compared of the $\tau_f = 30$ $[s]$ on the τ-timeline where it is originally defined, as $\alpha(\tau) > 1$ for the majority of the trajectory. Note that the formulation incorporates time-varying and non-smooth bounds, allowing us to consider bounds on the states and flat output space by iteratively modifying $\alpha_\pm^{(i)}(\tau)$.

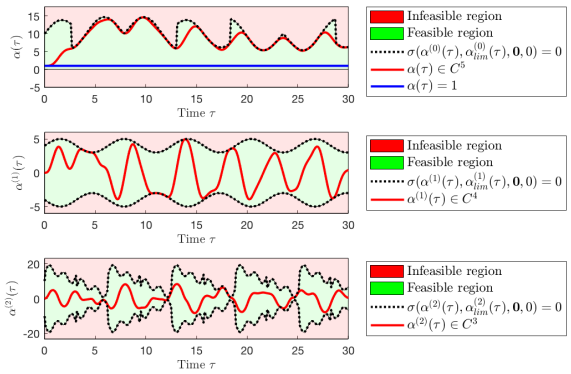

Fig. 4. Maximising $\alpha(\tau) \in C^5$ with discontinuous periodic constraints.

(iv) Convex constraints in $\boldsymbol{\gamma}(\tau)$: It should be noted that the constraints on the first and second derivatives on $\boldsymbol{\gamma}(\tau)$ with respect to the t-timeline are convex in $\mathcal{X}$ by Faá di Bruno's formula (20). As such, the incorporation of

$$\sigma(\boldsymbol{\gamma}_t^{(i)}(\tau)) \leq 0 \quad i \in \{1, 2\} \tag{33}$$

in the formulation (32) results in a convex QP for which we may still find the desired time-optimal solutions. This is particularly useful for the considered systems, as it allows the bounding of the velocities and accelerations in the global frame. However, incorporating the convex nonlinear constraints typically requires interior-point methods (or equivalent), which converge slowly and to visibly poor solutions. It is therefore advised to solve the problem with affine constraints, dealing with any nonlinear constraint by an iterative approach outlined in the next subsection.

(v) Non-convex constraints in $\boldsymbol{\gamma}(\tau)$ and $\{\mathbf{x}(t), \mathbf{u}(t)\}$: All higher derivative constraints on $\boldsymbol{\gamma}(\tau)$ with respect to the t-timeline are non-convex and may not be incorporated in the QP-formulation directly (32). Any attempt to do so results in non-convex constraints, with solutions depending on the initial conditions of the optimisation, optimal only in a local sense and typically solved with very slow convergence rates.

The affine convex constraints will often suffice, but conservative time-varying bounds on derivatives of $\boldsymbol{\gamma}(\tau)$ may be converted into constraints on $\alpha(\tau)$ using Cauchy-Schwartz inequality. This leads to a recursive definition of conservative bounds, with problems tending to becoming infeasible. Another approach is to include the non-convex constraints in a formulation which seeks to both maximise $J(\mathcal{X})$ and the space spanned by the bounds on $\alpha(\tau)$. This approach also resultsin problems prone to becoming infeasible.

Finally, as that the trajectory $\alpha(\tau) = 1$ $\forall i > \tau$ is followable, and the linear QP is relatively small, an iterative approach may be considered where the QP is solved and bounds on $\alpha(\tau)$ are incrementally changed on each iteration. This is made possible by the definition of the flatness equations, as the bounds may be evaluated on the t-timeline each point in time $\tau = \Delta\tau k$ without integration. If a nonlinear or non-convex signal is saturated for a specific

$\tau = \Delta\tau k$, all constraints on $\alpha(\tau)$ are changed incrementally at this time to decrease $\alpha(\Delta\tau k)$. Conversely, the bounds are relaxed if no signal is saturated at $\tau = \Delta\tau k$. This allows us to state that (1) the resulting trajectory satisfies the non-convex saturations down to a known error, and (2) it is time-optimal with respect to the resulting constraints on $\alpha(\tau)$.

VII. Numerical Examples

In all the following examples, we consider flat output trajectories $\boldsymbol{\gamma}(\tau)$ (blue), which with a nominal time-warping $\alpha^n(\tau) = 1 \ \ \forall\tau$ (blue), implies $t = \tau$ and a nominal trajectory $\boldsymbol{\gamma}^n(t) = \boldsymbol{\gamma}(\tau)$. The quadratic program is then formed to find a time-warping $\alpha^*(\tau)$ (red) such that the trajectory when evaluated on the t-timeline $\boldsymbol{\gamma}^*(t)$ (red) is time-optimal.

A. Time-optimal driving with time-varying bounds

Consider the two UGV models with parameters $h = 0.1$ $[m]$, $r = 0.05$ $[m]$, $m = 0.3$ $[kg]$, $J = 0.1$ $[kg/m/s^2]$, $J_1 = J_2 = 10^{-2}$ $[kg/m/s^2]$, such that the kinetic tensor of the $SE(2)$-configured system may be written

$$\mathbb{I} = \text{diag}\{0.3, 0.1, 0.1\}.$$

Having designed a simple lane (see Figure 5, black dashed), we let the UGVs start and finish in $(x_{\mathcal{G}}(0), y_{\mathcal{G}}(0)) = (x_{\mathcal{G}}(\tau_f), y_{\mathcal{G}}(\tau_f)) = (0, 0)$. A minimum snap trajectory, $\boldsymbol{\gamma}(\tau)$, is then generated by the CPO-method, consisting of eight polynomials with $\deg(\boldsymbol{\gamma}(\tau)) = 8$ and $\tau_f = 19.9$ $[s]$ (blue).

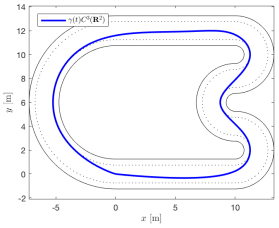

Fig. 5. A feasible trajectory $\gamma^n(\tau) \in C^3(\mathbb{R})$ on a track with margins.

The task is then to find a complementing time-warping $\alpha(\tau) \in C^{M-1}(\mathbb{R})$, with $M = 2$ in the constrained case and $M = 3$ in the unconstrained case. To this end, we define

$$\boldsymbol{\gamma}_+^{(1)}(\tau) = -\boldsymbol{\gamma}_-^{(1)}(\tau) = \begin{bmatrix} 5 + 2\sin(\tau) \\ 5 + 2\sin(\tau) \end{bmatrix}, \ \ \boldsymbol{\gamma}_r^{(1)}(\tau) = 13^2,$$
$$\boldsymbol{\gamma}_+^{(2)}(\tau) = -\boldsymbol{\gamma}_-^{(1)}(\tau) = \begin{bmatrix} \infty \\ \infty \end{bmatrix}, \ \ \boldsymbol{\gamma}_r^{(2)}(\tau) = \infty,$$
$$\alpha_+^{(0)}(\tau) = 5, \ \ \alpha_-^{(0)}(\tau) = 0, \alpha_+^{(1)}(\tau) = -\alpha_-^{(1)}(\tau) = 10\forall\tau,$$
$$\alpha_+^{(2)}(\tau) = -\alpha_-^{(2)}(\tau) = 5, \ \alpha_+^{(3)}(\tau) = -\alpha_-^{(3)}(\tau) = 5\forall\tau,$$

Running the optimisation program with a discretisation of $\Delta\tau = 0.01$ on $\tau \in [0, 19.9]$, an optimal $\alpha^*(\tau)$ (red) is found which allows evaluation of a time-optimal flat trajectory on the t-timeline, where it is compared to a nominal $\alpha^n(\tau) = 1$ (see Figure 6). Given the constraints on the flat output derivatives, it turns out that $\alpha^*(\tau) \geq \alpha^n(\tau) \ \ \forall\tau$, implying that the terminal time t_f occurs earlier on the t-timeline with the optimised time-warping $\alpha^*(\tau)$ given the constraints. Indeed, the trajectory is completed in $t_f|_{\alpha^*} = 12.2$ $[s]$ using the optimal time-warping, as opposed to the $t_f|_{\alpha^n} = \tau_f = 19.9$ $[s]$ of using the nominal CPO-generated trajectory. The dominating sinusoidal bounds on $\boldsymbol{\gamma}^{(1)}(\tau)$ are given with respect to the τ-timeline, and clearly not saturated in the original sub-optimal trajectory. However, when incorporating the optimal time-warping $\alpha^*(\tau)$, the constraints are no-longer sinusoidal on the t-timeline as $\alpha^*(\tau) \neq 0 \ \ \forall\tau$. Nevertheless the constraints are met, and the velocity bounds are visibly saturated at almost all times while retaining smoothness, making $\gamma^*(t)$ followable by Theorem 1.

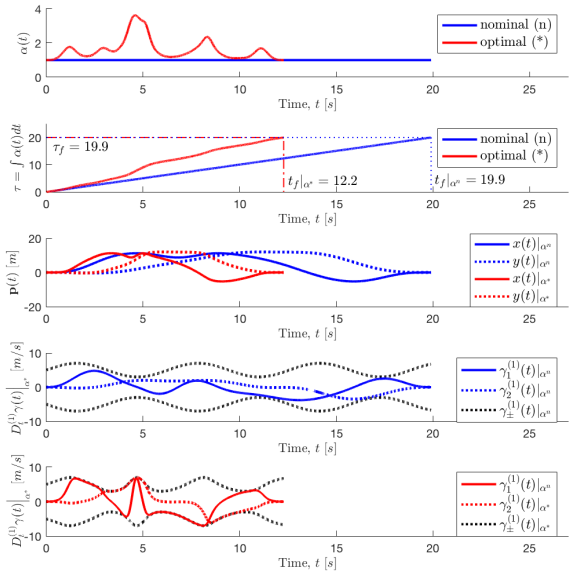

Fig. 6. A nominal $\alpha^n(\tau) = 1 \ \ \forall\tau$ and maximised $\alpha(\tau) \in C^3(\mathbb{R})$ subject to sinusoidal constraints.

When controlling the two dynamical systems along the optimal trajectory, using feed-forward from the flatness equations and a simple nonlinear stabilising feedback law, the positional trajectories (blue and red corresponding to $\mathbf{p}(t)|_{\alpha^n}$ and $\mathbf{p}(t)|_{\alpha^*}$, respectively) are followed nicely by the $SE(2)$ configured UGV and the UGV subject to differential constraints, but the corresponding attitude responses are completely different along the trajectories (see Figure 7).

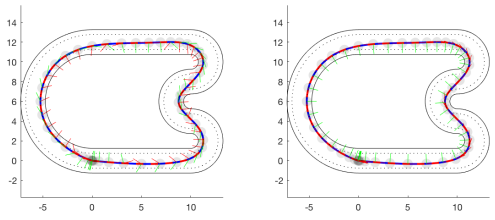

Fig. 7. The nominal trajectory $\boldsymbol{\gamma}^n(\tau)$ (blue) and simulated motion along the optimised flat output trajectory $\boldsymbol{\gamma}^*(t)$ with the $SE(2)$ configured UGV (left) and the non-holonomically constrained UGV (right).

B. Time-optimal looping with non-convex constraints

In the second example, we consider the $SE(3)$ configured UAV with rigid body dynamics defined by the tensor

$$\mathbb{I} = \text{diag}\{m, m, m, J_{xx}, J_{yy}, J_{zz}\}$$

with $m = 0.027$ $[kg]$, $J_{xx} = J_{yy} = 1.66 \cdot 10^{-5}$ $[kg/m/s^2]$, $J_{zz} = 2.93 \cdot 10^{-5}$ $[kg/m/s^2]$. The rotor-speed to thrust map, and implicitly motor dynamics, are defined by the parameters $l = 0.046$ $[m]$, $k = 2.2 \cdot 10^{-8}$ $[N \cdot m \cdot s^2]$ and $b = 2 \cdot 10^{-9}$ $[N \cdot m \cdot s^2]$. This choice of parameters correspond to the Crazyflie 2.0 UAV [22] and implies the quadcopter reaching a stable hovering state when $\Omega_i(t) \approx 1780$ $[rad/s]$. The system is to follow a trajectory $\boldsymbol{\gamma}(\tau)$ on $\tau \in [0, 8]$ [s], defined

$$\boldsymbol{\gamma}(\tau) = -[\sin(\pi\tau/4), \sin(\pi\tau/2), \cos(\pi\tau/2), -\pi\tau/4]^T.$$

resulting in the looping manoeuvre illustrated in Figure 8.

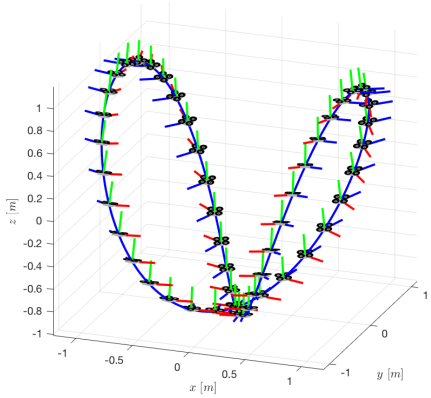

Fig. 8. A looping manoeuvre with $\gamma(\tau) \in C^\infty(\mathbb{R}^4)$.

Similar to the UGV example, we find a complementing time-warping $\alpha(\tau) \in C^{M-1}(\mathbb{R})$, with $M = 3$. As the primary saturations in the UGV system is in the motor dynamics, we consider a saturation on the rotor speeds $\boldsymbol{\Omega}$, with $\boldsymbol{\sigma}(\boldsymbol{\Omega}(t)) \leq \mathbf{0}$ defined by a rectangular saturation with

$$\begin{aligned} \boldsymbol{\Omega}_+(t) &= 2.5 \cdot 10^3 \cdot [1, 1, 1, 1]^T \quad \forall t, \\ \boldsymbol{\Omega}_-(t) &= 5 \cdot 10^2 \cdot [1, 1, 1, 1]^T \quad \forall t, \\ \boldsymbol{\Omega}_r(t) &= \infty \quad \forall t \end{aligned}$$

corresponding to physical limitations of the rotors [22]. Note that these constraints are both highly nonlinear and non-convex, requiring the iterative optimization approach. In addition, we include a constant linear bound on the positional derivatives on the form $\boldsymbol{\sigma}(\boldsymbol{\gamma}^{(1)}(t)) \leq \mathbf{0}$, defined by

$$\boldsymbol{\gamma}_+^{(1)}(t) = -\boldsymbol{\gamma}_-^{(1)}(t) = [5, 5, 5, \infty]^T, \quad \boldsymbol{\gamma}_r^{(1)}(t) = \infty.$$

Running the optimisation program with $\Delta\tau = 0.01$ on $\tau \in [0, 8]$, a solution $\alpha^*(\tau)$ (red) is found and subsequently compared to a nominal $\alpha^n(\tau) = 1$ on the t-timeline (see Figure 9). The transit time is more than halved in using $\alpha^*(\tau)$, with $t_f|_{\alpha^*} = 3.8$ compared to $t_f|_{\alpha^n} = 8.0$. All constraints are satisfied, with the bounds in velocity hit at two points in time, and the rotor speed bounds residing close to their upper bound, reaching it in approximately 0.5 $[s]$ due to the smoothness condition and system inertia.

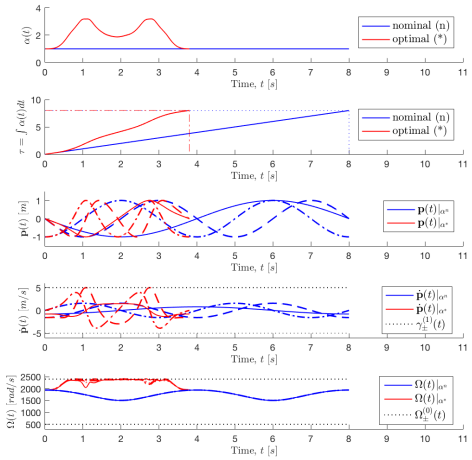

Fig. 9. The nominal- (blue) and computed time-optimal (red) trajectories for the $SE(3)$-configured UAV during the looping manoeuvre.

Controlling the UAV along this trajectory using the AGAS nonlinear geometric control law in [28], we see that the trajectory is not only followed to near perfection as expected from Theorem 1, but the UAV reaches an upside-down attitude in order to complete the manoeuvre - a highly volatile state which would be difficult to reach if relying on single-point linearization. Indeed, if only considering velocities and attitudes of the systems, it is clear that a nonlinear MPC formulation would either require refactorisation of the system at very high rates, or a very high number of partitions if using the explicit form. In our formulation, it is sufficient to consider a high order integrator in finding the time-warping by Theorem 1 (see Figure 10).

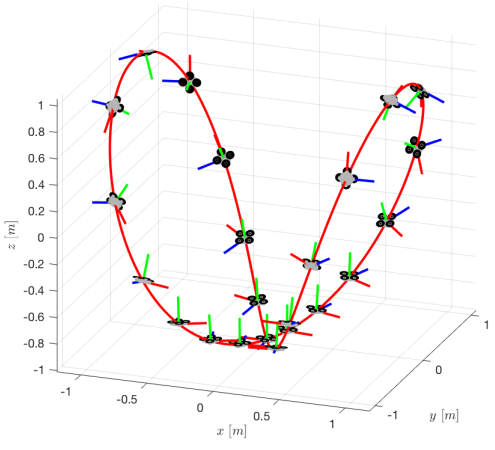

Fig. 10. Following the time-warped trajectory $\boldsymbol{\gamma}^*(t) \in C^3(\mathbb{R}^4)$ with the $SE(3)$-configured UAV during the looping manoeuvre.

VIII. CONCLUSIONS

In this paper, we consider time-optimal movement of differentially flat systems along known paths $\boldsymbol{\gamma}(\tau)$ in the flat output space. We presented a time-warping transformation of the trajectory in order to find a complementary trajectory $\alpha(\tau)$ which warps the trajectory to achieve time-optimal motion provided sufficient smoothness of $\boldsymbol{\gamma}(\tau)$. This was done using convex optimisation, and an iterative approach was presented to deal with higher order non-convex constraints by a gradual expansion and contraction of the $\alpha(\tau)$ derivative bounds. The iterative method yields time-optimal solutions with respect to the position and velocity constraints, as well as the resulting bounds on the $\alpha(\tau)$ derivatives.

Two examples were given using the CPO method to generate an nominal flat output trajectory $\boldsymbol{\gamma}(\tau)$. The first with UGVs configured on $SE(2)$, both with and without differential constraints, where movement was fundamentally constrained by time varying bounds on the system velocities. A second example was given with the rotor speed controlled UAV configured on $SE(3)$, constrained only by the rotor speeds of the system. Our method only yields locally optimal solutions for the latter problem, as it is non-convex due to the rotor speed constraints, but still generates a followable trajectory which significantly speeds up the transition time along $\boldsymbol{\gamma}(\tau)$. It should also be noted that the method is not restricted to rigid-body dynamics, but could be considered for any differentially flat system by Definition 1.

While this approach is very useful for efficient time-optimal planning, many possible improvements may be explored to better deal with the non-convex constraints on the flat output trajectory derivatives. Future avenues of research could also include combining the CPO with the time-warping in an iterative manner for simultaneously finding $\boldsymbol{\gamma}(\tau)$ and $\alpha(\tau)$. In addition, experiments should be done with the method implemented in a real-time application. This could initially be done with offline generation of the time-warping, and later online with an MPC-approach with a sufficiently long prediction horizon to preserve smoothness of $\alpha(\tau)$.

ACKNOWLEDGMENT

The author expresses his sincere thanks to Professor Anders Robertsson at Lund University for support and helpful discussions, and Professor Emeritus Karl Johan Åström for inspiring the paper by his inherent curiosity and desire to see the UAV perform looping manoeuvres.

REFERENCES

[1] J.-C. Latombe, *Robot motion planning*. Springer Science & Business Media, 2012, vol. 124.

[2] S. M. LaValle, *Planning algorithms*. Cambridge university press, 2006.

[3] N. Slegers, J. Kyle, and M. Costello, "Nonlinear model predictive control technique for unmanned air vehicles," *Journal of Guidance Control and Dynamics*, vol. 29, no. 5, pp. 1179–1188, 2006.

[4] C. Goerzen, Z. Kong, and B. Mettler, "A survey of motion planning algorithms from the perspective of autonomous UAV guidance," *Journal of Intelligent and Robotic Systems*, vol. 57, no. 1-4, p. 65, 2010.

[5] K. Berntorp and F. Magnusson, "Hierarchical predictive control for ground-vehicle maneuvering," in *American Control Conference (ACC), 2015*. IEEE, 2015, pp. 2771–2776.

[6] S. M. LaValle, "Rapidly-exploring random trees: A new tool for path planning," *Computer Science Dept., Iowa State University*, no. TR 98-11, 1998.

[7] Y. Kuwata, J. Teo, G. Fiore, S. Karaman, E. Frazzoli, and J. P. How, "Real-time motion planning with applications to autonomous urban driving," *IEEE Transactions on Control Systems Technology*, vol. 17, no. 5, pp. 1105–1118, 2009.

[8] O. Arslan, K. Berntorp, and P. Tsiotras, "Sampling-based algorithms for optimal motion planning using closed-loop prediction," in *Robotics and Automation (ICRA), 2017 IEEE International Conference on*. IEEE, 2017, pp. 4991–4996.

[9] R. Tedrake, I. R. Manchester, M. Tobenkin, and J. W. Roberts, "LQR-trees: Feedback motion planning via sums-of-squares verification," *The International Journal of Robotics Research*, vol. 29, no. 8, pp. 1038–1052, 2010.

[10] P. Töndel, T. A. Johansen, and A. Bemporad, "An algorithm for multi-parametric quadratic programming and explicit MPC solutions," *Automatica*, vol. 39, no. 3, pp. 489–497, 2003.

[11] C. Richter, A. Bry, and N. Roy, "Polynomial trajectory planning for aggressive quadrotor flight in dense indoor environments," in *Proceedings of the International Symposium on Robotics Research (ISRR)*, 2013.

[12] ——, "Polynomial trajectory planning for aggressive quadrotor flight in dense indoor environments," in *Robotics Research*. Springer, 2016, pp. 649–666.

[13] M. Fliess, J. Lévine, P. Martin, and P. Rouchon, "Flatness and defect of non-linear systems: introductory theory and examples," *International journal of control*, vol. 61, no. 6, pp. 1327–1361, 1995.

[14] ——, "A Lie-Bäcklund approach to equivalence and flatness of nonlinear systems," *IEEE Transactions on automatic control*, vol. 44, no. 5, pp. 922–937, 1999.

[15] M. van Nieuwstadt, M. Rathinam, and R. M. Murray, "Differential flatness and absolute equivalence," in *Decision and Control, 1994., Proceedings of the 33rd IEEE Conference on*, vol. 1. IEEE, 1994, pp. 326–332.

[16] A. D. Lewis and R. M. Murray, "Configuration controllability of simple mechanical control systems," *SIAM Journal on control and optimization*, vol. 35, no. 3, pp. 766–790, 1997.

[17] M. Rathinam and R. M. Murray, "Configuration flatness of lagrangian systems underactuated by one control," *SIAM journal on control and optimization*, vol. 36, no. 1, pp. 164–179, 1998.

[18] M. Greiff, "Studies of configuration controllability and differential flatness in control-affine systems," *Department of Automatic Control, Lund University, Sweden*, 2017. [Online]. Available: https://github.com/mgreiff/pre-prints/blob/master/preprintB.pdf

[19] M. Fliess, J. Lévine, P. Martin, F. Ollivier, and P. Rouchon, "A remark on nonlinear accessibility conditions and infinite prolongations," *Systems & control letters*, vol. 31, no. 2, pp. 77–83, 1997.

[20] R. M. Murray, Z. Li, S. S. Sastry, and S. S. Sastry, *A mathematical introduction to robotic manipulation*. CRC press, 1994.

[21] M. Bangura, M. Melega, R. Naldi, and R. Mahony, "Aerodynamics of rotor blades for quadrotors," *arXiv preprint arXiv:1601.00733*, 2016.

[22] M. Greiff, "Modelling and control of the crazyflie quadrotor for aggressive and autonomous flight by optical flow driven state estimation," *Department of Automatic Control, Lund University, Sweden, MSc Thesis TFRT-6026 ISSN 0280-5316*, 2017.

[23] D. Mellinger and V. Kumar, "Minimum snap trajectory generation and control for quadrotors," in *Robotics and Automation (ICRA), 2011 IEEE International Conference on*. IEEE, 2011, pp. 2520–2525.

[24] O. Dahl and L. Nielsen, "Torque-limited path following by online trajectory time scaling," *IEEE Transactions on Robotics and Automation*, vol. 6, no. 5, pp. 554–561, 1990.

[25] O. Dahl, "Path constrained motion optimization for rigid and flexible joint robots," in *Robotics and Automation, 1993. Proceedings., 1993 IEEE International Conference on*. IEEE, 1993, pp. 223–229.

[26] F. Debrouwere, W. Van Loock, G. Pipeleers, Q. T. Dinh, M. Diehl, J. De Schutter, and J. Swevers, "Time-optimal path following for robots with convex–concave constraints using sequential convex programming," *IEEE Transactions on Robotics*, vol. 29, no. 6, pp. 1485–1495, 2013.

[27] S. Roman, "The formula of Faa di Bruno," *The American Mathematical Monthly*, vol. 87, no. 10, pp. 805–809, 1980.

[28] T. Lee, M. Leoky, and N. H. McClamroch, "Geometric tracking control of a quadrotor UAV on SE(3)," in *Decision and Control (CDC), 2010 49th IEEE Conference on*. IEEE, 2010, pp. 5420–5425.